Fluid Phase Equilibria 426 (2016) 83–94

Contents lists available at ScienceDirect

Fluid Phase Equilibria

journal homepage: www.elsevier.com/locate/fluid

Solid–liquid equilibrium of binary and ternary systems formed by ethyl laurate, ethyl palmitate and n-decane: Experimental data and thermodynamic modeling

Maria Dolores Robustillo [a], Duclerc Fernandes Parra [b], Antonio José de Almeida Meirelles [c], Pedro de Alcântara Pessôa Filho [a, *]

[a] Department of Chemical Engineering, Engineering School, University of São Paulo (USP), Caixa Postal 61548, 05424-970, São Paulo, SP, Brazil
[b] Nuclear and Energy Research Institute (IPEN), Center for Chemical and Environmental Technology (CQMA), Av. Prof. Lineu Prestes, 2242, 05508-000, São Paulo, SP, Brazil
[c] Department of Food Engineering (DEA), School of Food Engineering (FEA), University of Campinas (UNICAMP), Rua Monteiro Lobato, 80, 13083-862, Campinas, SP, Brazil

ARTICLE INFO

Article history:
Received 30 October 2015
Received in revised form
17 January 2016
Accepted 22 January 2016
Available online 27 January 2016

Keywords:
Solid–liquid equilibrium
Ethyl esters
Decane
Binary systems
Ternary systems

ABSTRACT

The solid–liquid equilibrium phase diagrams of binary and ternary mixtures formed by n-decane and the fatty acid ethyl esters ethyl laurate and ethyl palmitate were studied through differential scanning calorimetry (DSC). Phase change properties of polymorphs were obtained by resolving the thermograms into the corresponding overlapping peaks through a fitting analysis with a Gaussian function. The binary systems show immiscibility in solid phase. The system formed by ethyl laurate and n-decane presents two peritectic transformations, which were also observed in the ternary phase diagram. Equilibrium data were thermodynamically modeled using different models for liquid phase non-ideality and considering different polymorphs in solid phase. The results of modeling are in good agreement with the eutectic behavior of the system formed by ethyl palmitate and n-decane. However, higher discrepancies were observed if no peritectic behavior for the binary system formed by ethyl laurate and n-decane is considered. The results obtained in this work constitute another step forward to enhance the understanding and description of the complex behavior of biodiesel/diesel mixtures at low temperatures.

1. Introduction

The use of pure biodiesel at low temperatures is limited by the crystallization of its components, which affects cold–flow properties [1–3] and may lead to flow assurance problems and damage of engines. Thus, the use of blends of biodiesel and conventional hydrocarbon-based diesel has become increasingly common. The sources of biomass, along with the alcohol used in the production process, determine the composition of the biodiesel. High melting temperature compounds, such as stearic acid (C18:0), or medium melting temperature compounds, such as oleic acid (C18:1) and linoleic acid (C18:2), occur in appreciable amounts in most sources. Other acids such as lauric acid (C12:0) and myristic acid (C14:0) are found in large proportions in coconut oil, while palmitic acid (C16:0) is the main component of palm oil [4]. The formulation, transport and storage of diesel/biodiesel blends can be improved if the solid liquid equilibrium (SLE) of these blends is known. However, experimental equilibrium data of such mixtures is still scarce. Concerning pure compounds, Knothe and Dunn [2] conducted an extensive evaluation of melting points of fatty acids and esters, summarized the experimental data available in literature and published new data obtained by differential scanning calorimetry (DSC). Phase diagrams of some binary mixtures of fatty acid methyl and ethyl esters are presented in Lockemann and Schlünder [5], Boros et al. [6] and Costa et al. [7,8]. Robustillo et al. [9–12] presented *liquidus* lines of ternary systems formed by several ethyl esters (ethyl laurate, ethyl palmitate, ethyl oleate, ethyl myristate and ethyl stearate). Mixtures of biodiesel were analyzed by Imahara et al. [4] and Coutinho et al. [13]. Kouakou et al. [14] and Carareto et al. [15] studied the influence of pressure in pure methyl esters and binary mixtures of ethyl esters, respectively. However, only a few solid liquid phase diagrams of mixtures of fatty acid esters and

---

[*] Corresponding author.
E-mail address: pedro.pessoa@poli.usp.br (P.A. Pessôa Filho).

http://dx.doi.org/10.1016/j.fluid.2016.01.044
0378-3812/

Table 1
Sources and properties of the pure compounds used in the experiments.

Chemical name	Source	Mass fraction purity	Formula	Molar mass/g·mol^{-1}	$T_{f,\,Lit}$/K[c]	Functional groups					v_i
						$-CH_3$	$-CH_2$	c$-CH_2$	c$-$CH	$-CH_2COO$	
Ethyl laurate (EL)	Sigma Aldrich	$\geq$0.98	$C_{14}H_{22}O_2$	228.4		2	10	0	0	1	8.860
Ethyl palmitate (EP)	Sigma Aldrich	$\geq$0.99	$C_{18}H_{36}O_2$	284.5		2	14	0	0	1	11.390
N-decane (DE)	Sigma Aldrich	$\geq$0.99	$C_{10}H_{22}$	142.3	243.51 [26]	2	8	0	0	0	6.325
Indium[a]	Mettler Toledo[b]	0.9999	In	114.82	429.75						
Naphthalene[a]	Merck	$\geq$0.99	$C_{10}H_8$	128.17	353.35 [27]						
Cyclohexane[a]	Merck	$\geq$0.99	C_6H_{12}	84.16	279.81 [27]						

[a] Compounds used only for calibrating the DSC apparatus.
[b] Calibration standard.
[c] Literature onset melting temperature.

components of conventional diesel have been obtained. The exceptions are the works by Collinet and Gmehling [16], where mixtures of ethyl myristate and p-xylene were studied, and the works of Benziane et al. [17,18], where solid–liquid equilibrium of fatty acid methyl esters with heavy alkanes and aromatics were studied. Recently, we have studied the solid–liquid equilibrium behavior of binary and ternary mixtures of ethyl esters and a naphthenic compound (dodecylcyclohexane) [19]. To the best of our knowledge, no work was found in the literature studying the solid–liquid phase behavior of ethyl esters and light alkanes.

This work comprises the experimental determination of solid–liquid equilibrium (SLE) of binary and ternary mixtures of ethyl laurate and ethyl palmitate, two ethyl esters commonly found in biodiesel [4], and n-decane, a low molecular weight paraffin present in conventional diesel [20]. Mixtures were analyzed by differential scanning calorimetry (DSC), which allows the simultaneous determination of both the *liquidus* and the *solidus* lines. Properties of polymorphs of ethyl laurate and ethyl palmitate were formerly obtained [19] by integration of corresponding heating thermograms following a method previously proposed by Canotilho et al. [21]. The polymorphism of n-decane is also addressed. The solid–liquid equilibrium was described by considering different models for the liquid phase behavior (ideal mixture, Flory–Huggins [22] and UNIFAC-Dortmund [23–25]), and considering different polymorphs in the solid phase. To the best of our knowledge, no other experimental data set for the binary systems containing these ethyl esters and n-decane, as well as for the corresponding ternary systems, was reported in literature.

2. Experimental section

2.1. Materials

Sources and purities of the compounds used in this work – n-decane (1), ethyl laurate (2) and ethyl palmitate (3) – are presented in Table 1. The differential scanning calorimeter (model DSC 822e, Mettler Toledo) was calibrated using indium, naphthalene, cyclohexane and n-decane. Their properties are also presented in Table 1. Literature onset melting temperatures for calibration were obtained from Refs. [26,27]. Masses were measured in a Sartorius balance with 220 g weighing capacity and 0.1 mg readability.

2.2. Methods

The procedure to obtain the temperature profile through Differential Scanning Calorimetry (DSC) was similar as used in previous works [9–12,19] and comprises the following steps:

(1) A sample was weighed (between 2 and 5 mg) and placed in hermetic aluminum pans inside the DSC furnace.
(2) This sample was heated to approximately 15 K above the highest pure component melting temperature.
(3) The sample was cooled (at a cooling rate of 1 K min^{-1}) to approximately 25 K below the lowest pure component melting point and equilibrated at that temperature for 5 min.

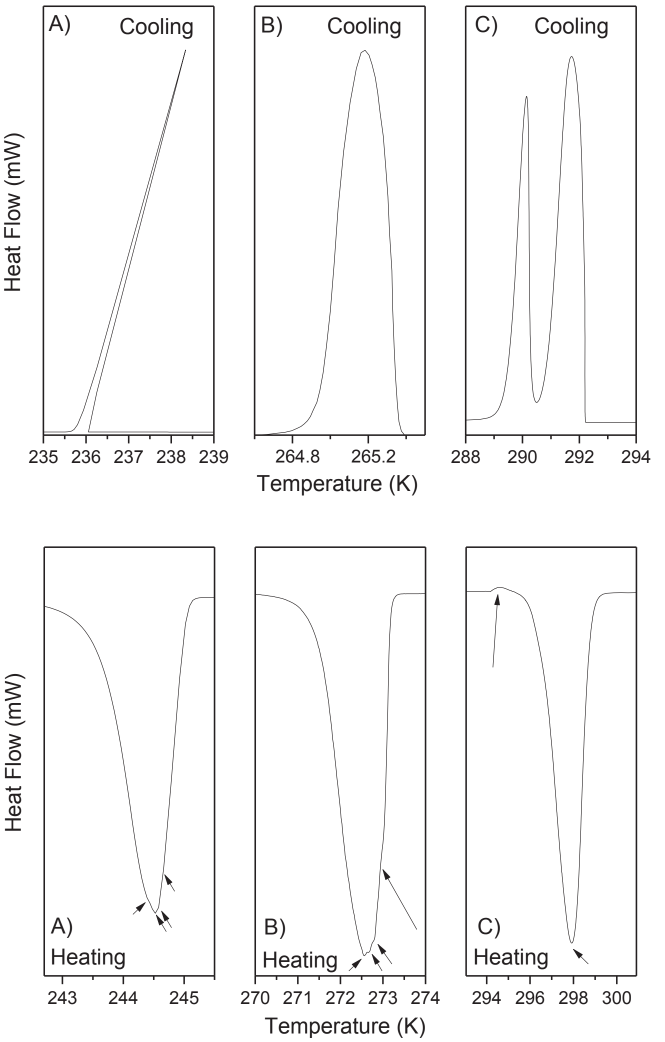

Fig. 1. Thermograms of the compounds studied in this work: A) n-decane (1); B) ethyl laurate (2); C) ethyl palmitate (3).

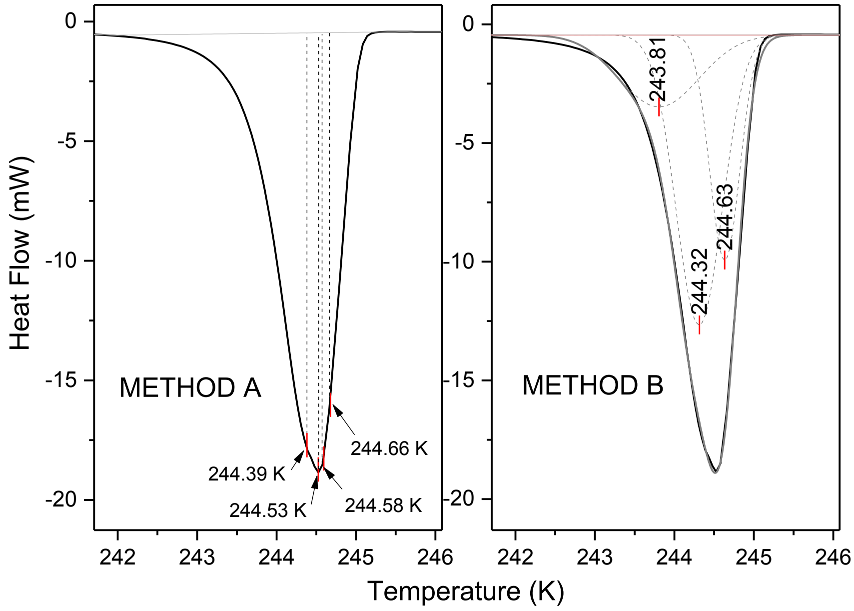

Fig. 2. Comparison of integration methods A and B for n-decane: – – original thermogram; — calculated total Gaussian function.

(4) The sample was then heated (at a heating rate of 1 K min^{-1}) until complete melting.

Nitrogen (99.99% purity) was fed at a rate of 50 mL min^{-1}. The transition temperature corresponding to the phase change (melting temperature) was considered to be the transition peak apex, which is located by the intersection of the tangents to the peak slopes. It corresponds to the absolute minimum of the heat flow in the heating thermogram for every phase change signal considered. The melting temperature generally matches the highest temperature transition observed in the thermogram.

3. Modeling

The *liquidus* line temperature was calculated through a phase stability analysis following a procedure previously presented [28]. For simple eutectic systems, the stability analysis results in the usual solid–liquid equations. However, if peritectic reactions take place, the *liquidus* temperature can be calculated by considering that the peritectic compound formed by the reaction between compounds *i* and *j* corresponds to a 1:1 compound:

$$\left(\frac{\Delta_{fus}G_i}{RT}+\ln\left(a_i^L\right)\right)+\left(\frac{\Delta_{fus}G_j}{RT}+\ln\left(a_j^L\right)\right)+\ln\left(K_{ij}\right)=0 \tag{1}$$

where $\Delta_{\text{fus}}\text{G}$ is the Gibbs energy change on fusion, K_{ij} is the equilibrium constant of the peritectic reaction between *i* and *j*. Considering that $\varDelta H^0$ and $\varDelta S^0$ (the standard enthalpy and entropy of the peritectic reaction) do not depend on temperature:

$$\ln(\text{K}_{\text{ij}})=-\frac{\Delta\text{G}^0}{\text{RT}}=-\frac{\Delta H^0}{R}\left[\frac{1}{\text{T}}\right]+\frac{\Delta\text{S}^0}{\text{R}}=\frac{\text{b}}{\text{T}}+\text{a} \tag{2}$$

where a and b are constants.

The activity of the compounds in liquid phase was calculated through three approaches. The first one is to consider that the liquid phase is ideal. The second one considers that the liquid phase non-ideality is given by the Flory–Huggins equation [22]:

$$\ln\left(a_i^L\right)=1+\ln(\varphi_i)-\upsilon_i\sum_j\frac{\varphi_j}{\upsilon_j}+\upsilon_i\left(\sum_j\chi_{ij}\varphi_j-\sum_j\sum_{k>j}\chi_{jk}\varphi_j\varphi_k\right) \tag{3}$$

Volume fractions are calculated through:

Table 2
Melting properties of the studied compounds determined by DSC estimated from heating thermograms.

Compound	Polymorph	Method A			Method B		
		T_f/K	ΔH_f/kJ mol^{-1}	$\Delta\text{H}_{\text{f total}}$/kJ mol^{-1}	T_f/K	ΔH_f/kJ mol^{-1}	$\Delta\text{H}_{\text{f total}}$/kJ mol^{-1}
n-Decane	DE-1	244.39	15.36		243.80	6.40	
	DE-2	244.53	15.36 + 5.79 = 21.15		244.32	6.40 + 14.89 = 21.29	
		244.58	15.36 + 5.79+2.36 = 23.51				
	DE-3	244.66	15.36 + 5.79+2.36 + 5.19 = 28.70	28.70	244.63	6.40 + 14.89+7.54 = 28.83	28.83
Ethyl laurate	EL-1	272.56	25.18		272.23	23.73	
	EL-2	272.66	25.18 + 11.20 = 36.38		272.66	23.73 + 10.54 = 34.27	
	EL-3	273.00	25.18 + 11.20+2.56 = 38.94	38.94	272.95	23.73 + 10.54+4.00 = 38.27	38.27
Ethyl palmitate	EP-1	294.63	0.24				
	EP-2	297.93	53.03				

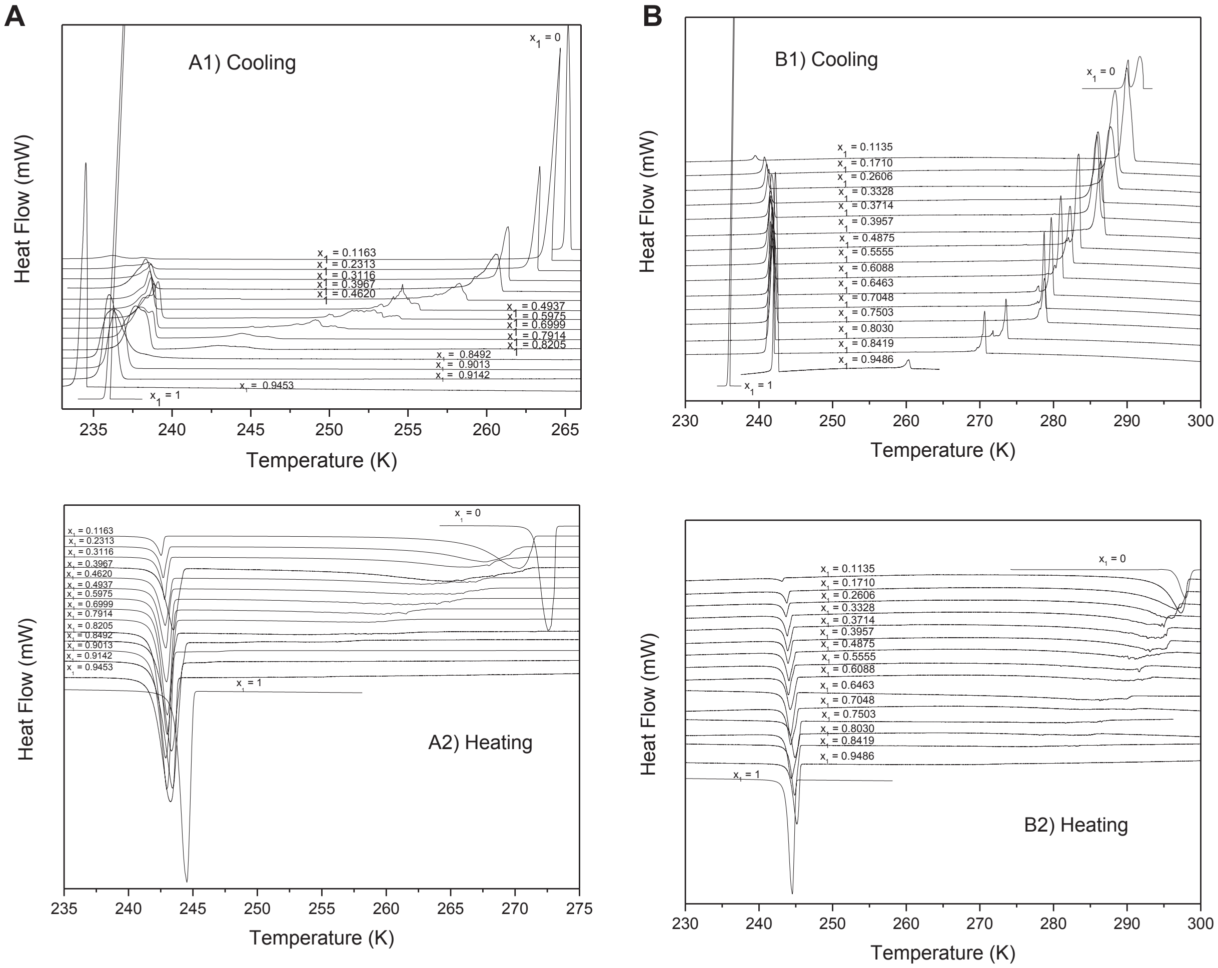

Fig. 3. Thermograms of the binary mixtures studied in this work: A) n-decane (1) + ethyl laurate (2); B) n-decane (1) + ethyl palmitate (3).

$$\varphi_i = \frac{x_i v_i}{\sum_j x_j v_j} \tag{4}$$

and the summations are carried out over all compounds. To calculate volume fractions, UNIFAC-Dortmund volume parameters were used as molar volumes [23].

The third approach is to consider that liquid phase non-ideality is given by the group contribution model UNIFAC-Dortmund [23–25]. UNIFAC group interaction parameters were obtained from Gmehling et al. [23].

4. Results and discussion

4.1. Experimental data

4.1.1. Pure compounds

Fig. 1 shows the cooling and heating thermograms of the studied compounds. To reduce the influence of kinetic effects, only heating thermograms were used to determine numerical values. Polymorphism of ethyl laurate and ethyl palmitate was studied previously [9,10,29,30]. The behavior of n-decane was studied by Broadhurst [31], who analyzed the solid phase behavior of normal paraffins. Although n-alkane molecules have a simple molecular structure, their solid phase behavior can be unusual. According to Broadhurst [31], different crystal structures can be found in solid phases of n-paraffins with more than nine carbon atoms in the chain: orthorhombic, hexagonal, triclinic and monoclinic. Those structures are combined with the so called rotator solid phase α (which is less ordered than a crystal, but more ordered than the melted compound) and the non-rotating solid phase β, a denser phase of lower crystallization temperature and higher stability.

According to Sirota et al. [32], n-paraffins follow a definite sequence when crystallizing. Let us define the orthorhombic rotator phase as R_I, the hexagonal rotator phase as R_{II}, the triclinic rotator phase as R_{III}, and the monoclinic rotator phase as R_{IV}. According to Sirota et al. [32] the general phase sequence is liquid → R_{II} → R_I → crystal in shorter chain lengths and liquid → R_{IV} → R_{III} → crystal in chains with more than 27 carbon atoms. Broadhurst [31] states that the non-rotating phase β with the triclinic crystal structure is observed for n-paraffin of even carbon number lower than 24, which includes n-decane. Rotating phases α were not observed for paraffins with even carbon number. This means that just one polymorph was identified by Broadhurst [31] for n-decane. However, Smith [33] showed evidence of polymorphism in hexadecane ($C_{16}H_{34}$) and octadecane ($C_{18}H_{38}$). Recently, techniques such as standard or modulated DSC, X-Ray diffraction and polarized light optical microscopy have shown that rotator phases occur in eicosane ($C_{20}H_{42}$) [32,34] and n-docosane ($C_{22}H_{46}$) [32] on cooling. Since different transitions were observed very close to each other in the thermograms of n-decane, as shown in Fig. 1 during heating,

Table 3
Experimental (solid + liquid) equilibrium data for the systems: A) Decane (1) + ethyl laurate (2) and B) Decane (1) + ethyl palmitate (3), for liquid mole fraction x, temperature T, and pressure p = 0.1 MPa[a].

Decane (1) + Ethyl laurate (2)

x_1	T_t/K[b]	T_e/K	T_p/K	T_f/K	Solid phase
0				272.95	(2)
0.1163	242.54			270.43	(2)
0.2313	242.80			268.05	(2)
0.3116	242.85			266.19	(2)
0.3967	243.48			264.53	(2)
0.4620	242.86			262.84	(2)
0.4937	242.92		256.23	262.54	(2)+(P_1)
0.5975		242.96	256.60	261.55	(P_1)+(P_2)
0.6999		243.05	256.32	259.75	(P_2)
0.7914		243.22	255.62	258.46	(P_2)
0.8205		242.89		257.51	(P_2)
0.8492		243.06		254.71	(P_2)
0.9013		243.25		247.13	(P_2)
0.9142		243.13		245.63	(P_2)
0.9453				243.86	(P_2)+(1)
1				244.63	(1)

Decane (1) + Ethyl palmitate (3)

x_1	T_e/K	T_f/K	Solid phase
0		297.93	(3)
0.1135	244.10	296.70	(3)
0.1710	243.65	295.35	(3)
0.2606	243.75	294.74	(3)
0.3328	244.37	293.66	(3)
0.3714	243.95	292.85	(3)
0.3957	243.95	292.45	(3)
0.4875	244.05	287.85	(3)
0.5555	243.70	286.42	(3)
0.6088	244.15	284.95	(3)
0.6463	244.52	285.82	(3)
0.7048	244.25	281.75	(3)
0.7503	244.89	280.96	(3)
0.8030	244.35	278.25	(3)
0.8419	244.84	275.99	(3)
0.9486	245.16	264.75	(3)
1		244.63	(1)

[a] Standard uncertainties u are u(T) ≈ 0.5 K for melting and 0.3 K for the other transitions, u(x) ≈ 0.0002.

[b] T_e = eutectic temperature; T_t = transition temperature; T_f = melting temperature.

Table 4
Experimental (solid + liquid) equilibrium data for the system n-decane (1) + ethyl laurate (2) + ethyl palmitate (3) for liquid mole fraction X, temperature T, and pressure p = 0.1 MPa[a].

Sample	x_2	x_3	T_e/K[b]	T_p/K	T_f/K
1	0.1019	0.0936	242.6	247.3	272.5
2	0.2135	0.0902	242.7	253.2	271.6
3	0.2908	0.1135	242.5	256.3	272.1
4	0.3831	0.1222	242.5	259.3	272.1
5	0.5043	0.0935	242.5	262.0	269.9
6	0.5975	0.0962	242.3	263.9	268.1
7	0.6740	0.1117	241.7	264.9	269.7
8	0.7447	0.1376	241.8	266.4	272.1
9	0.1221	0.1968	242.5	249.3	276.5
10	0.2506	0.2072	242.6	256.5	278.4
11	0.2687	0.2294	242.6	257.2	279.3
12	0.4232	0.1798	242.6	261.0	279.6
13	0.5079	0.1913	242.5	263.4	276.5
14	0.5852	0.1987	242.3	265.2	277.1
15	0.6524	0.1892	242.2	266.6	276.5
16	0.1062	0.3200	242.6	248.8	283.9
17	0.2102	0.3008	242.5	256.4	283.5
18	0.3128	0.2923	242.6	259.7	284.3
19	0.3899	0.2842	242.5	261.7	283.0
20	0.4902	0.2964	242.3	264.4	282.1
21	0.5310	0.2765	242.3	265.0	281.5
22	0.1120	0.3815	242.4	250.1	287.1
23	0.3303	0.3744	242.2	261.0	285.7
24	0.3427	0.4267	242.1	262.4	288.2
25	0.4126	0.3957	242.0	263.6	286.5
26	0.4904	0.4181	241.3	265.9	285.1
27	0.2381	0.4857	242.2	260.0	288.9
28	0.1192	0.5580	242.2	254.4	290.3
29	0.1846	0.5397	242.2	258.3	290.6
30	0.2803	0.5342	242.1	263.2	288.1
31	0.1286	0.6284	242.2	256.5	291.6
32	0.1916	0.6233	242.1	261.3	291.3
33	0.1587	0.6791	242.3	261.4	293.5

[a] Standard uncertainties u are u(T) ≈ 0.5 K for melting temperatures and ≈0.3 K for eutectic and peritectic temperatures, u(x) ≈ 0.0003.

[b] T_e = eutectic temperature; T_t = transition temperature; T_f = melting temperature.

the existence of a rotating phase α cannot be *a priori* discarded.

As previously mentioned [19], different types of functions may be used to resolve superimposed peaks in DSC thermograms. The

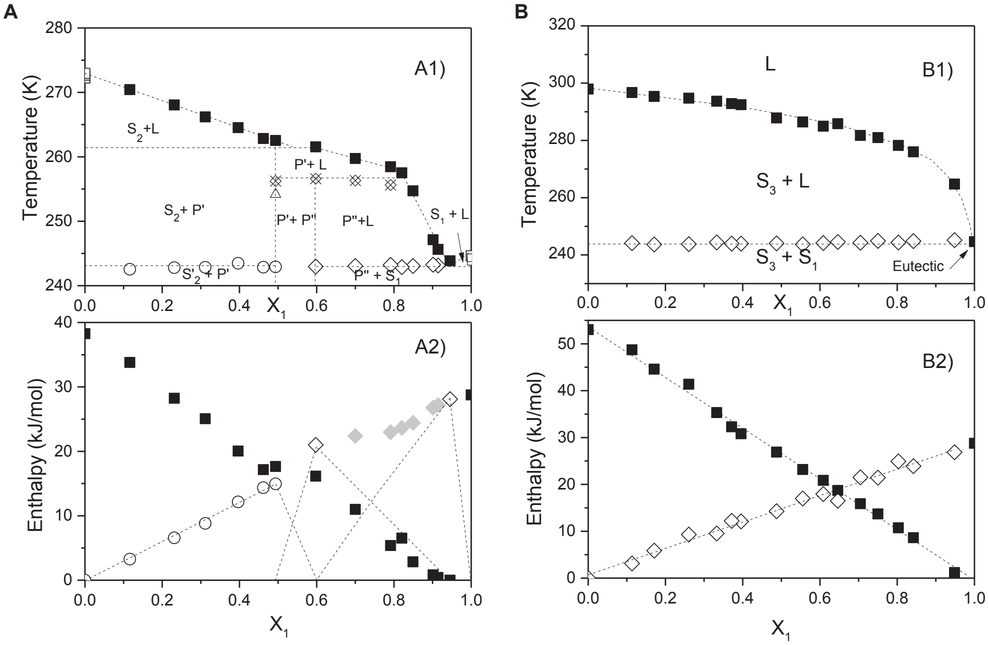

Fig. 4. Phase diagram (above) and Tamman's diagram (below) for the binary systems: A) n-decane (1) + ethyl laurate (2); B) n-decane (1) + ethyl palmitate (3): ■ – melting; ◇ – eutectic; ⊠ – peritectic; ○ – solid–solid transition; ◆ – total enthalpy of overlapped transitions.

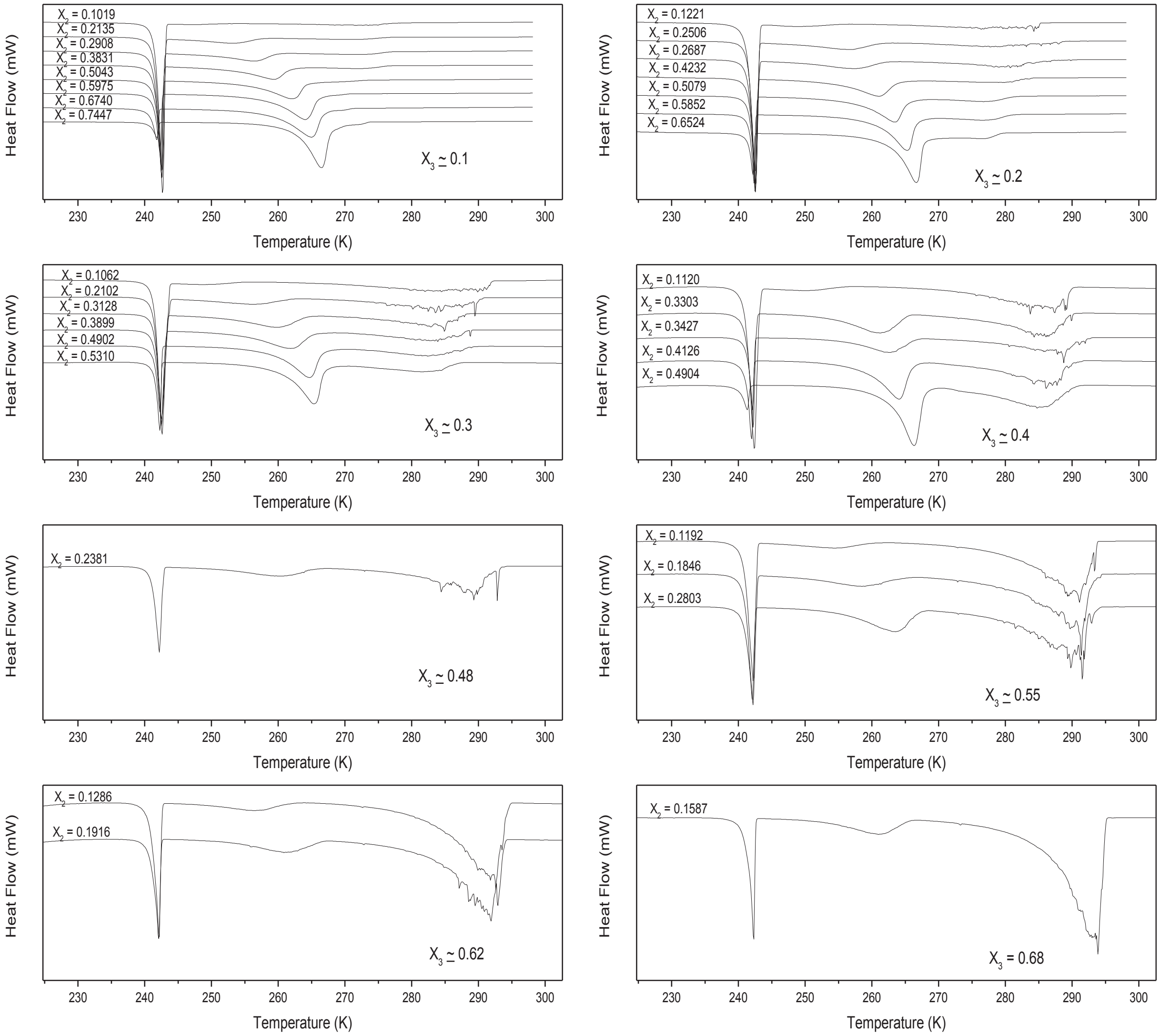

Fig. 5. Thermograms of the ternary system n-decane (1) + ethyl laurate (2) + ethyl palmitate (3).

most common are the perpendicular drop analysis (method A) and the Gaussian function multiple peak fitting, proposed by Canotilho et al. [21] (method B). Each fitted Gaussian curve represents a possible polymorph. Fig. 2 shows the integration of n-decane thermograms through both methods.

Table 2 summarizes the melting properties of n-decane and includes the values obtained for ethyl laurate and ethyl palmitate [19] for comparison. According to Gill et al. [35], for overlapped peaks the most stable polymorph would be the one with the highest melting temperature. The more stable the polymorph, the lower the differences in melting enthalpy obtained through both methods. Similar values of total enthalpy for the most stable polymorph were obtained through both methods. Thus, the use of method B is preferred, because it filters transitions that do not follow a normal distribution and may be ascribed to kinetic effects, lattice defects or simply noise [19]. The values of melting temperature of the considered most stable polymorph of n-decane (DE-3) and of its total transition enthalpy are in good agreement with published data [36,37]. However, the values presented here are slightly higher, as we consider peak temperature (244.63 K) equivalent to melting temperature and not to the experimental onset (243.58 K) or endset (245.02 K) temperatures of the total phase change peak.

4.1.2. Binary mixtures

The binary system formed by ethyl laurate (2) and ethyl palmitate (3) was studied previously [9]. Fig. 3A shows the thermograms for the system formed by n-decane (1) and ethyl laurate (2). Sharper peaks around 243 K are observed in heating thermograms. They correspond to the eutectic transition. However, in cooling thermograms differences in temperatures are more significant, which might indicate that this event corresponds not only to the eutectic transition but also to the presence of different solid phases. Although these small differences in temperatures could be due to kinetic effects, the cooling rate used is very low (1 K min^{-1}), for which kinetic effects are probably negligible.

For n-decane mole fractions higher than 0.4, noise is observed in the highest temperature peak in both cooling (Fig. 3A1) and heating thermograms (Fig. 3A2). This noise reduces around n-decane mole fractions of 0.82. Similar behavior was observed by Müller et al. [38] for systems containing other paraffins such as n-hexane and n-dodecane. These authors attributed this phenomenon either to heat storage effects of the pan and sensor or to small pressure variations. These fluctuations do not correspond to real equilibrium states and hinder the determination of meting temperature. Hillert [39] points out that controlling all state variables may be difficult in this case. Pressure control is difficult for solid systems, especially during a phase change, as it may increase deformations and internal stresses, which affect heat flow. Although those effects are usually negligible, it is possible to find situations in which their influence in heat flow is considerable. Previous results [19], as well as results obtained by Müller et al. [38] for systems formed by other paraffins, show that this phenomenon is more significant when the mixture is formed by light compounds. Since the lower is the molecular weight of a compound (in a homologous series), the greater is its vapor pressure, such noise is likely to be related to very small pressure changes occurring locally in the piece of sample. Moreover, this noise is observed for compositions that can be related to the formation of a peritectic compound, as will be shown later in the corresponding phase diagram.

To facilitate the integration of thermograms to determine temperature transitions, melting peaks of complex thermograms were treated through a Fast Fourier Transform (FFT) function, as described in previous work [19].

The eutectic composition for the system n-decane and ethyl laurate corresponds to a n-decane mole fraction of approximately 0.95. This condition is characterized by a single peak in the thermogram.

For the system formed by n-decane (1) and ethyl palmitate (3), Fig. 3B, each thermogram exhibits two main peaks. The peak with higher temperature corresponds to the melting of the component with higher melting temperature, and the lowest peak corresponds to the eutectic transition. In cooling thermograms (Fig. 3B1), differences in temperature are within the experimental uncertainty, which indicates that the presence of different solid phases is less probable.

Table 3 shows the experimental data for the binary mixtures. Temperatures correspond to the absolute minimum heat flow obtained after using a smoothing function. Standard deviations were 0.5 K for melting and 0.3 K for peritectic and eutectic transitions. Data shown in Table 3 are average values.

Fig. 4 presents the proposed phase diagrams for the binary systems (top) and the enthalpy of transition as a function of concentration (bottom). These latter plots are known as Tamman's plots. Lines are drawn to guide the eyes to possible phase distributions: only scattered points are actual experimental data. The system n-decane and ethyl laurate (Fig. 4A) shows an increase in the enthalpy of the lower temperature peaks obtained during heating as the mole fraction of n-decane increases. At n-decane mole fractions of about 0.5, 0.6 and 0.82, different breaks in the linearity of the enthalpy of the lower temperature peaks are observed. Melting enthalpy also breaks its linearity at those points. Since the energy required for the eutectic reaction is proportional to the amount of liquid formed in the mixture, those breaks can be related to peritectic reactions, for which the liquid phase is consumed and the solid phase composition changes. This hypothesis agrees with the inflection points observed in the *liquidus* line at temperatures around 261.3 K and 256.2 K.

The increasing of the enthalpy for n-decane mole fractions up to 0.5 may be related to the melting of the peritectic compound P'. At n-decane mole fraction of 0.5, the amount of P′ in the sample decreases and a new solid phase (P″) is increasingly formed. The maximum enthalpy for this phase is observed at n-decane mole fraction of 0.6. By increasing n-decane mole fraction, the melting of the eutectic compound starts and reaches its maximum at n-decane mole fraction of 0.95. The gray diamonds shown in Tamman's plot (Fig. 4A2) actually depict the total enthalpy of overlapped effects (reduction of the amount of P″ and increase of the amount of the eutectic one). Once the eutectic composition is reached, the enthalpy decreases. Tamman's plot does not indicate the existence of regions of partial miscibility for this system.

Fig. 4B shows the phase diagram of the binary system n-decane and ethyl palmitate. This system seems to be a simple eutectic one. This fact indicates that the components are not miscible in the solid phase. In Tamman's plot, no linearity break occurs in the eutectic solid phase enthalpy or in the melting peak. This fact is in agreement with the simple eutectic behavior of the solid phase. Tamman's plot does not indicate the existence of regions of partial miscibility for this system either.

4.2. Ternary mixtures

Table 4 presents the experimental data of the ternary system formed by n-decane (1), ethyl laurate (2) and ethyl palmitate (3), and Fig. 5 presents the corresponding thermograms. A sharp endothermic peak at an average temperature of 242.3 K is observed in all thermograms. This peak corresponds to the eutectic transition. As in previous work [19], the use of the smoothing function was necessary to determine the melting temperature.

The eutectic composition is defined as the lowest temperature

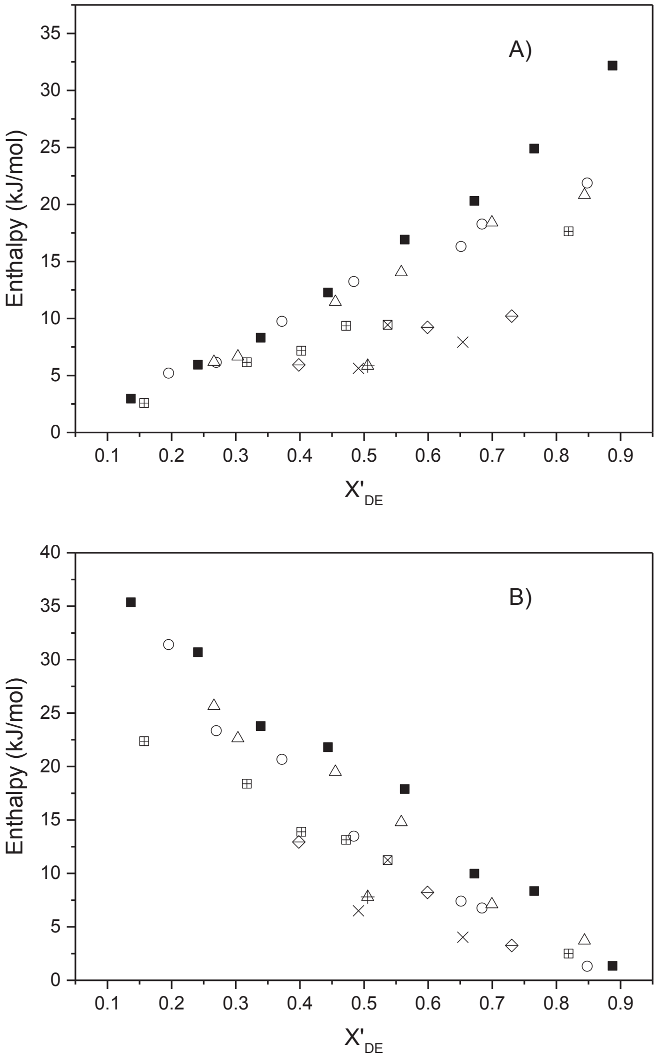

Fig. 6. Tamman's diagram for the ternary system: A) eutectic transition; B) peritectic transition; X'_{DE}: composition of n-decane base free of ethyl palmitate; ■ – X_3 ~ 0.1; ○ – X_3 ~ 0.2; Δ- X_3 ~ 0.3; ⊞ – X_3 ~ 0.4; ⊠- X_3 ~ 0.48; ◇- X_3 ~ 0.55; × – X_3 ~ 0.62; △- X_3 ~ 0.68.

at which a liquid phase can be observed. Tamman's plot for a binary mixture presents a maximum at the eutectic composition and a minimum at the extremes of the phase diagram [40]. In a ternary system, Tamman's diagram should be a 3D representation. However, since ethyl palmitate has a significantly higher melting temperature, it has no appreciable influence on the eutectic transition. Thus, Tamman's diagram can be represented in 2D considering the compositions of n-decane and ethyl laurate in an ethyl palmitate-free basis. Fig. 6A presents Tamman's diagram for the eutectic transition of the ternary system. Small differences in linearity are due to small differences in ethyl palmitate composition for experimental points with the same nominal ethyl palmitate fraction. In this case, just one maximum and one minimum were observed for all constant compositions of ethyl palmitate studied. The experimental compositions with ethyl palmitate mole fraction of around 0.10 present lower temperatures. Since Tamman's diagrams show an increase in the enthalpy up to n-decane mole fractions of around 0.90 (in ethyl palmitate-free basis), with no minimum, the eutectic composition of the ternary system cannot be determined in this way. A possible inference is that the eutectic has a mole fraction of ethyl palmitate lower than 0.10. However, the eutectic composition can be determined graphically from the *liquidus* line phase diagram (Fig. 7) according to the procedure proposed by Ozawa and Matsuoka [41]. Temperatures of polymorphs with higher melting points were used for representation. In a ternary diagram, points of any straight line passing through a vertex of the triangle (e.g. EP) and intercepting the opposite side (e.g., line DE-EL) are the *loci* of mixture compositions in which the proportion of components corresponding to the other two vertices (DE and EL) is constant. Thus, considering the side DE-EL of Fig. 7 (corresponding to the binary system formed by n-decane and ethyl laurate), the eutectic composition (E) has a n-decane mole fraction of around 0.95 (represented by the point $E_{DE\text{-}EL}$). Mixtures with constant proportion of n-decane and ethyl laurate will lie in the line EP-$E_{DE\text{-}EL}$. Similar reasoning is applied to the lines DE-$E_{EL\text{-}EP}$ and EL-$E_{EP\text{-}DE}$. All these lines (EP-$E_{DE\text{-}EL}$, DE-$E_{EL\text{-}EP}$ and EL-$E_{EP\text{-}DE}$) are expected to pass close to the ternary eutectic point. The interception of them provides an inference of the composition of the ternary eutectic. In this case, the ternary eutectic has mole fractions of n-decane, ethyl laurate and ethyl palmitate around 0.93, 0.06 and 0.01, respectively. The temperature of the *liquidus line* increases as the fraction of ethyl palmitate increases, as expected from the melting temperatures of pure compounds.

In a ternary system, the peritectic temperature may change depending on the composition, without modification of the phases involved. Thus, according to the Gibbs Phase rule, the peritectic transition is monovariant (1 degree of freedom). The peritectic transition was observed in the binary system formed by n-decane and ethyl laurate. From the side DE-EL of the triangle, the line that joins the vertex EP with the compositions of binary peritectics (mole fractions of ethyl laurate of 0.4 and 0.5, named P_B'' and P_B' respectively in Fig. 7) is the *locus* of system compositions with the same ratio of ethyl laurate and n-decane. Cooling thermograms of ternary samples below the mentioned straight line show four peaks during cooling. Thermograms of samples 12, 23, 32 and 33, with compositions defined in Table 4, are shown in Fig. 8. The highest temperature peak corresponds to the crystallization of the solid, mainly composed by ethyl palmitate. The following peak at lower temperature represents the crystallization of another solid, mainly composed by ethyl laurate. This solid reacts with the surrounding liquid and forms the peritectic compound. Finally, the eutectic is formed at the lowest temperature (between 235 and 240 K). This peak unfolds into two peaks in some cases. This phenomenon was also observed for binary mixtures, and may be attributed to solid–solid transitions involving n-decane. If the composition is over the mentioned straight line, only three peaks are observed. This is

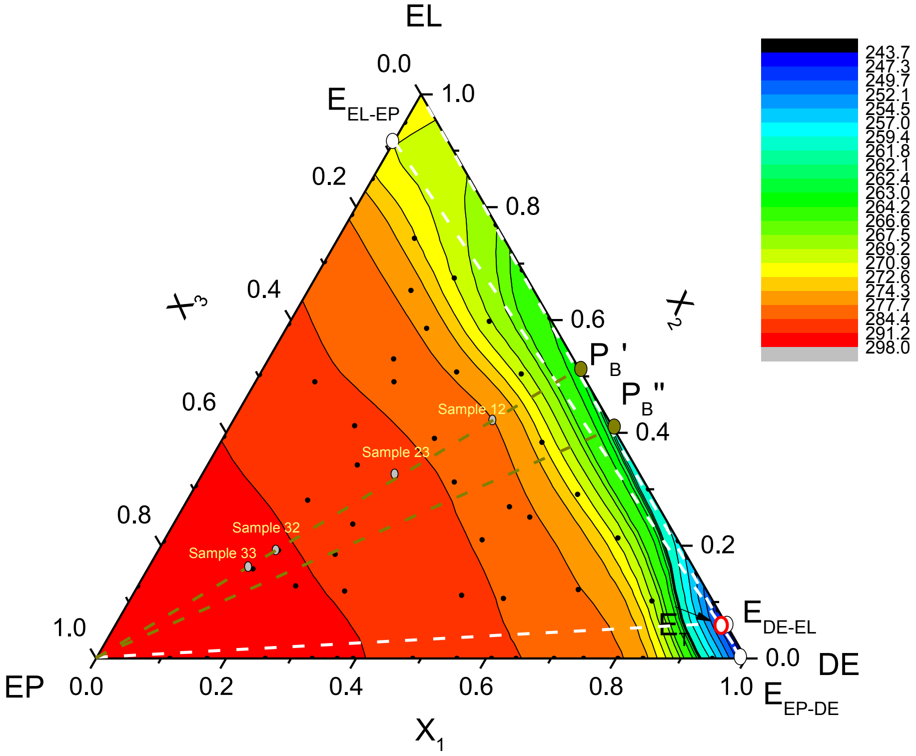

Fig. 7. Experimental phase diagram of n-decane (DE) + ethyl laurate (EL) + ethyl palmitate (EP): $E_{DE\text{-}EL}$, $E_{EP\text{-}DE}$ and $E_{EP\text{-}DE}$ are the binary eutectics; P_B' and P_B'' are binary peritectics.

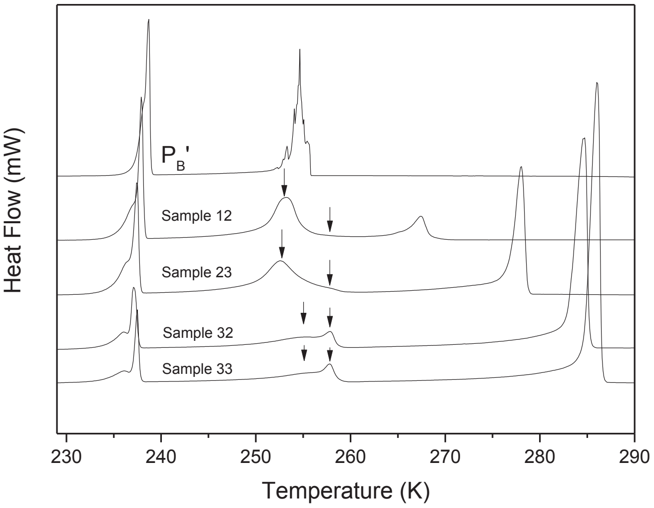

Fig. 8. Thermograms under cooling of some ternary mixtures exhibiting the peritectic reaction.

because the binary peritectic reaction is already completed.

Fig. 6B presents the enthalpy of the peritectic reaction as a function of the composition of n-decane and ethyl laurate in the ternary system, in ethyl palmitate-free basis. A decrease in the peritectic enthalpy when n-decane mole fraction increases is observed. This can be related to the fact that the lower the amount of ethyl laurate solid, the lower the amount of peritectic that will be formed. Nevertheless, it cannot be confirmed that the analyzed mixtures with the maximum enthalpy correspond to the ternary peritectic composition, as their melting temperatures are higher than the maximum peritectic temperature observed in Fig. 9 (around 266 K). Moreover, if the considered peritectic temperature is extrapolated to a mole fraction of n-decane equal to zero, the resulting temperature (266.01 K) is lower than melting temperature of pure ethyl laurate (272.95 K) or the mixture of ethyl laurate and ethyl palmitate with a mole fraction of ethyl palmitate 0.10 (269.16 K). This fact confirms the presence of the peritectic compound. The peritectic composition is probably defined by the intersection between EP-P_B' line and the *liquidus* line with temperature of approximately 266 K.

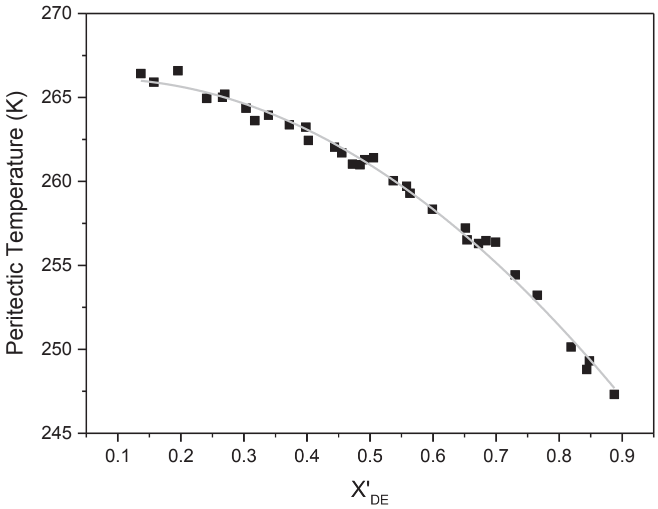

Fig. 9. Variation of peritectic temperature according to the composition of n-decane base free of ethyl palmitate.

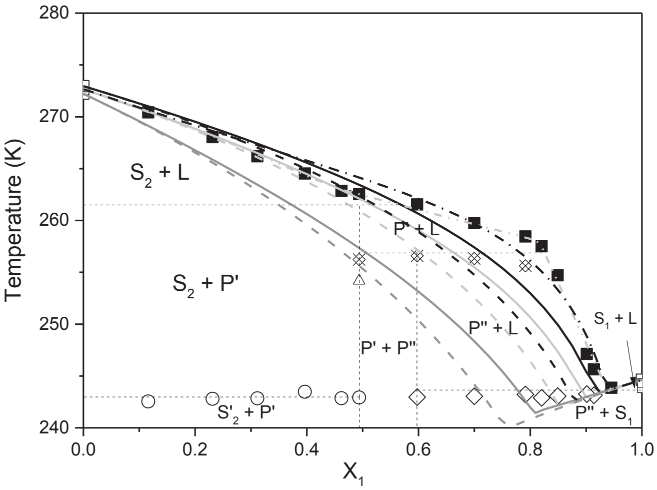

Fig. 10. Phase diagrams of the binary mixture n-decane (1) and ethyl laurate (2): ■ – liquidus line, experimental; ◇ – experimental eutectic; -·- – liquidus line Flory–Huggins modeling; ·····: Flory-Huggins-Peritectic; – – liquidus line UNIFAC-Dortmund modeling; - - – liquidus line ideal. Gray: LA-1+DE-3; Light gray: LA-2+DE-3; Black: LA-3+DE-3.

4.3. Thermodynamic modeling

The thermodynamic modeling was carried out by considering either that the liquid phase is ideal or that the liquid-phase non-ideality can be described by the Flory–Huggins equation [22] or the UNIFAC-Dortmund model [23–25]. Results for the binary system formed by ethyl laurate and ethyl palmitate have already been presented in previous work [19]. Fig. 10 shows the modeling results for the system formed by n-decane and ethyl laurate, and Fig. 11 presents the modeling results for the system formed by n-decane and ethyl palmitate. Table 5 summarizes the properties of pure compounds, the parameters used for the modeling and the standard deviation (SD) between experimental and calculated values. The value of SD was obtained through the following equation:

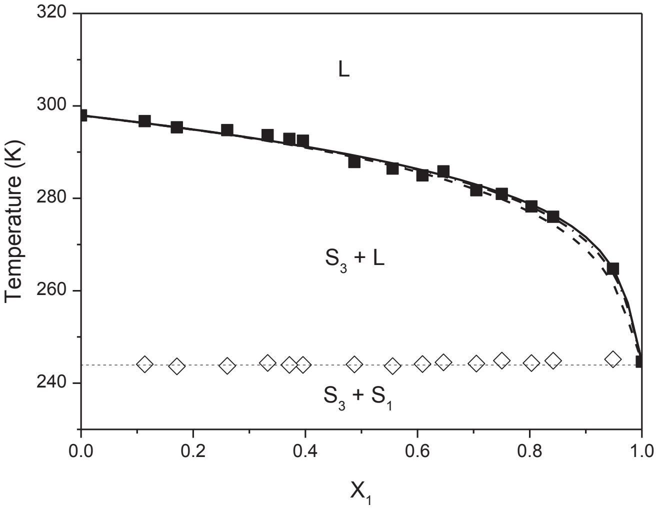

Fig. 11. Phase diagrams of the binary mixture n-decane (1) and ethyl palmitate (3): ■ – liquidus line, experimental; ◇ – experimental eutectic; -·- – liquidus line Flory–Huggins modeling; – – liquidus line UNIFAC-Dortmund modeling; - - – liquidus line ideal.

Table 5
Properties of parameters used for modeling and differences between experimental and predicted values.

System	Solid phase	Polymorphs	Name	Ideal[a]	Flory Huggins[a]	UNIFAC[a]	$\chi_{DE/EL}$	$\chi_{DE/EP}$	$\chi_{EL/EP}$
(DE)+(EL)	Eutectic	DE-3 + EL-1	A	9.63 (3.1[b])	1.02 (0.47[b])	8.23 (3.50[b])	0.2083		
	Eutectic	DE-3 + EL-2	B	6.51 (0.6[b])	1.38 (0.81[b])	3.97 (0.23[b])	0.1376		
	Eutectic	DE-3 + EL-3	C	5.01 (0.35[b])	1.63 (1.13[b])	2.65 (1.04[b])	0.1083		
	Peritectic	DE-3 + EL-2	D		0.40		0.0426		
(DE)+(EP)	Eutectic	DE-3 + EP-2	E	1.45	0.73	0.49		0.0394	
(DE)+(EL)+(EP)	Peritectic	DE-3+EL-2+ EP-2	F	2.20	2.77		0.0426	0.0394	−0.003

[a] Calculated SD, Eq. (5).
[b] Calculated SD considering only data for n-decane mole fractions from 0.1 to 0.5.

$$SD = \left(\frac{\sum_i \left(T_i^{calc} - T_i^{ex} \right)^2}{N} \right)^{1/2} \tag{5}$$

Two major aspects influence solid–liquid equilibrium calculations: the non-ideality of the liquid phase and the structure of the solid phase [19]. For the system formed by n-decane and ethyl laurate (Fig. 10), several modeling scenarios were studied by considering three different polymorphs of ethyl laurate. The use of properties of EL-2 (reference B in Table 5) and considering eutectic solid phase provides better agreement with experimental data for n-decane mole fractions lower than 0.5. Above that threshold, discrepancies are relevant. This can be explained by the existence of consecutive peritectic reactions.

Phase equilibrium was studied using the properties of EL-2 and considering liquid-phase non-ideality through the Flory–Huggins equation and peritectic formation (reference D in Table 5). The peritectic regions are described by the following equations:

$$\text{Peritectic 1:}\ \ln K = \frac{829.56}{T} - 1.7324 \tag{6}$$

$$\text{Peritectic 2:}\ \ln K = \frac{-3920.43}{T} + 16.9067 \tag{7}$$

The agreement of the calculated *liquidus* line is better than for all the previous cases, and only small discrepancies between experimental and calculated values were found.

A similar procedure was used to model the eutectic system formed by n-decane and ethyl palmitate (Fig. 11). The use of the polymorphs DE-3 and EP-2, with higher melting enthalpies (reference E in Table 5), resulted in a good description of the *liquidus* line, regardless of the description of the liquid phase.

As shown in Fig. 5, Flory–Huggins deviations are lower than those given by UNIFAC-Dortmund. This is due to the use of fitting parameters for Flory–Huggins results. Thus, differences between experimental and predicted values in case of UNIFAC-Dortmund predictive model are imputable to the presence of peritectic compounds for the system formed by n-decane and ethyl laurate, which were not considered in the predictions.

The *liquidus* line for the ternary system n-decane + ethyl

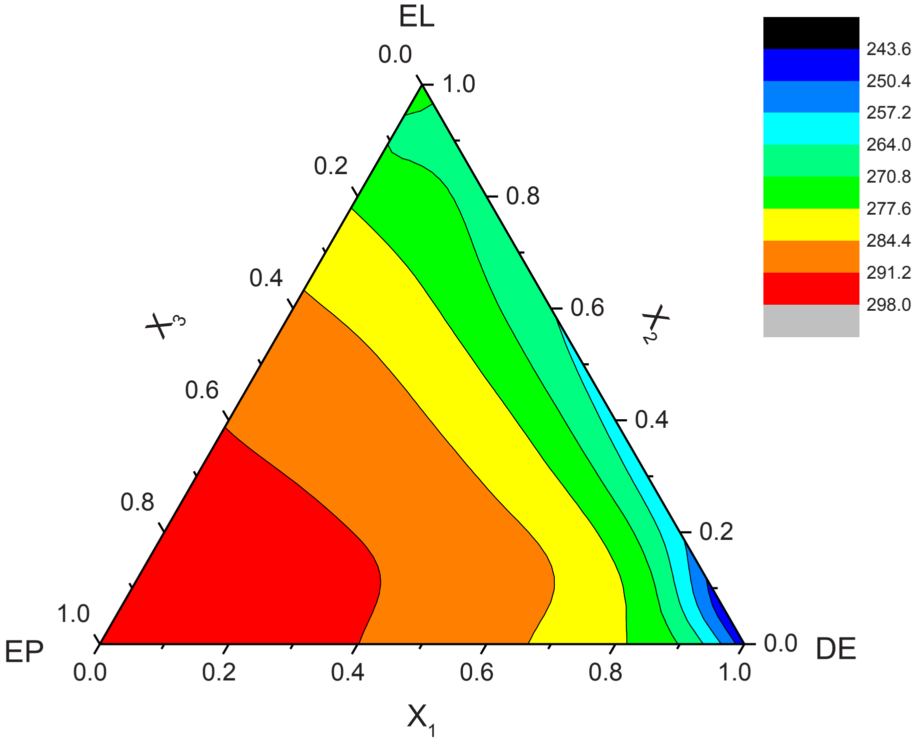

Fig. 12. Model prediction of ternary mixture n-decane (1) + ethyl laurate (2) + ethyl palmitate (3).

laurate + ethyl palmitate was also predicted using the Flory–Huggins model and considering solid phase immiscibility and peritectic reactions (reference F on Table 5). The interaction parameters were the same as those obtained for binary systems. The prediction of the *liquidus* temperature is satisfactory. However, no improvement was observed by considering the Flory–Huggins model compared to considering the ideal liquid phase. Fig. 12 presents results from ideal modeling for the ternary system. This Figure was constructed by considering the polymorphs EL-2, EP-2 and DE-3 for the ternary mixtures and the best predictions for representing binary systems: a) ethyl laurate + ethyl palmitate, EL-1 + EP-2 (liquid phase non-ideality determined by Flory Huggins, eutectic solid phase); b) n-decane + ethyl laurate: DE-3 + EL-2 (ideal liquid phase and peritectic solid phase); and c) n-decane + ethyl palmitate: DE-3 + EP-2 (liquid phase non-ideality determined by Flory Huggins, eutectic solid phase).

5. Conclusions

The solid–liquid equilibrium of binary and ternary systems containing n-decane, ethyl laurate and ethyl palmitate was experimentally determined through DSC. All binary systems present a definite eutectic point. For the system formed by n-decane and ethyl laurate, two peritectic transitions are also inferred. Cooling thermograms as well as the thermodynamic modeling helped to clarify this hypothesis. The binary peritectic transitions were also appreciated in cooling thermograms of ternary mixtures. Phase equilibrium was correlated using the Flory–Huggins model, and also predicted either using the UNIFAC-Dortmund model or considering liquid phase ideality. Differences between experimental and predicted values in case of UNIFAC-Dortmund model are imputable to the presence of peritectic compounds for the system formed by n-decane and ethyl laurate. Flory Huggins model considering solid phase immiscibility and the formation of peritectic compounds provided very good results. The results provided by predictive UNIFAC-Dortmund for the system formed by n-decane and ethyl palmitate are satisfactory. It demonstrates once again the reliability of that model for simple eutectic systems if the solid phase behavior is understood and the properties of the suitable polymorph are considered.

Acknowledgments

The authors thank the financial support of FAPESP (processes 2010/18355-1 and 2008/56258-8) and CNPq (process 150950/2014-4). The help of members of the laboratories ExTrAE (UNICAMP), Synthesis and Characterization of Polymers (CQMA/IPEN) and GenBio (USP) is also gratefully acknowledged, especially Flávio C. Matos, Patricia Tonon de Souza, Bruna Ligo, Eleosmar Gasparin and Luis F. M. Franco for assisting with the experimental work, and Mariana Costa and Natália Carareto for sharing their experiences of related works.

References

[1] R.O. Dunn, Crystallization behavior of fatty acid methyl esters, J. Am. Oil Chem. Soc. 85 (2008) 961–972.
[2] R.O. Dunn, Effects of high-melting methyl esters on crystallization properties of fatty acid methyl ester mixtures, Am. Soc. Agric. Biol. Eng. 55 (2012) 637–646.
[3] G.J. Maximo, M.C. Costa, J.A.P. Coutinho, A.J.A. Meirelles, Trends and demands in the solid–liquid equilibrium of lipidic mixtures, RSC Adv. 4 (2014) 31840.
[4] H. Imahara, E. Minami, S. Saka, Thermodynamic study on cloud point of biodiesel with its fatty acid composition, Fuel 85 (2006) 1666–1670.
[5] C.A. Lockemann, E.U. Schlünder, Solid-liquid phase equilibria of mixtures of methyl myristate and methyl palmitate, J. Chem. Eng. Data 38 (1993) 432–433.
[6] L. Boros, M.L.S. Batista, R.V. Vaz, B.R. Figueiredo, V.F.S. Fernandes, M.C. Costa, M.A. Krahenbuhl, A.J.A. Meirelles, J.A.P. Coutinho, Crystallization behavior of mixtures of fatty acid ethyl esters with ethyl stearate, Energy Fuels 23 (2009) 4625–4629.
[7] M.C. Costa, L.A.D. Boros, J.A.P. Coutinho, M.A. Krähenbühl, A.J.A. Meirelles, Low-temperature behavior of biodiesel: solid liquid phase diagrams of binary mixtures composed of fatty acid methyl esters, Energy Fuels 25 (2011) 3244–3250.
[8] M.C. Costa, L.A.D. Boros, M.L.S. Batista, J.A.P. Coutinho, M.A. Krähenbühl, A.J.A. Meirelles, Phase diagrams of mixtures of ethyl palmitate with fatty acid ethyl esters, Fuel 91 (2012) 177–181.
[9] M.D. Robustillo, D.F. Barbosa, A.J.A. Meirelles, P.A. Pessôa Filho, Solid liquid equilibrium in ternary mixtures of ethyl oleate, ethyl laurate and ethyl palmitate, Fluid Phase Equilib. 339 (2013) 58–66.
[10] M.D. Robustillo, D.F. Barbosa, A.J.A. Meirelles, P.A. Pessôa Filho, Solid-liquid equilibrium in ternary mixtures of ethyl laurate, ethyl palmitate and ethyl stearate, Fluid Phase Equilib. 358 (2013) 272–281.
[11] M.D. Robustillo, D.F. Barbosa, A.J.A. Meirelles, P.A. Pessôa Filho, Solid-liquid equilibrium in ternary mixtures of ethyl laurate, ethyl palmitate and ethyl myristate, Fluid Phase Equilib. 361 (2014), 361–188.
[12] M.D. Robustillo, D.F. Barbosa, A.J.A. Meirelles, P.A. Pessôa Filho, Solid-liquid equilibrium of binary and ternary mixtures containing ethyl oleate, ethyl myristate and ethyl stearate, Fluid Phase Equilib. 370 (2014) 85–94.
[13] J.A.P. Coutinho, M. Gonçalves, M.J. Pratas, M.L.S. Batista, V.F.S. Fernandes, J. Pauly, J.L. Daridon, Measurement and Modeling of Biodiesel Cold-Flow Properties, Energy Fuels 24 (2010) 2667–2674.
[14] A.C. Kouakou, K. Le Mapihan, J. Pauly, Solid–liquid equilibria under high pressure of pure fatty acid methyl esters, Fuel 109 (2013) 297–302.
[15] N. Carareto, M.C. Costa, A.J.A. Meirelles, J. Pauly, High pressure solid–liquid equilibrium of fatty acid ethyl esters binary systems, Fluid Phase Equilib. 382 (2014) 158–163.
[16] E. Collinet, J. Gmehling, Activity coefficient at infinite dilution, azeotropic data, excess enthalpies and solid–liquid-equilibria for binary systems of alkanes and aromatics with esters, Fluid Phase Equilib. 230 (2005) 131–142.
[17] M. Benziane, K. Khimeche, D. Trache, A. Dahmani, Experimental determination and prediction of (solid + liquid) phase equilibria for binary mixtures of aromatic and fatty acids methyl esters, J. Therm. Anal. Calorim. 114 (2013) 1383–1389.
[18] M. Benziane, K. Khimeche, A. Dahmani, S. Nezar, D. Trache, Experimental determination and prediction of (solid + liquid) phase equilibria for binary mixtures of heavy alkanes and fatty acids methyl esters, J. Therm. Anal. Calorim. 112 (2013) 229–235.
[19] M.D. Robustillo, A.J.A. Meirelles, P.A. Pessôa Filho, Solid-liquid equilibrium of binary and ternary systems formed by ethyl laurate, ethyl palmitate and dodecylcyclohexane: Experimental data and thermodynamic modeling, Fluid Phase Equilibria 409 (2016) 157–170.
[20] A.E. Buczynsky, Synthetic diesel fuel compositions, US Patent 2010/0287819 A1, 2009.
[21] J. Canotilho, F.S. Costa, A.T. Sousa, J.S. Redinha, M.L.P. Leitão, Melting curves of terfenadine crystallized from different solvents, J. Therm. Anal. Calorim. 54 (1998) 139–149.
[22] J.M. Prausnitz, R.N. Lichtenthaler, E.G. Azevedo, Molecular Thermodynamics of Fluid-phase Equilibria, third ed., Prentice Hall, New Jersey, 1999.
[23] J. Gmehling, J. Li, M. Schiller, A modified UNIFAC model. 2. Present parameter matrix and results for different thermodynamic properties, Ind. Eng. Chem. Res. 32 (1993) 178–193.
[24] J. Gmehling, J. Lohmann, A. Jakob, J. Li, R. Joh, A modified UNIFAC (Dortmund) model. 3. Revision and extension, Ind. Eng. Chem. Res. 37 (1998) 4876–4882.
[25] A. Fredenslund, R.L. Jones, J.M. Prausnitz, Group-contribution estimation of activity coefficients in nonideal liquid mixtures, AIChE J. 21 (1975) 1086–1099.
[26] DIPPR: Design Institute for Physical Properties Database.
[27] R. Sabbah, An Xu-wu, J.S. Chickos, M.L. Planas Leitão, M.V. Roux, L.A. Torres, Reference materials for calorimetry and differential thermal analysis, Thermochim. Acta 331 (1999) 93–204.
[28] D.F. Barbosa, P.A. Pessôa Filho, On the description of the liquidus line of systems presenting peritectic reactions, Fluid Phase Equilib. 337 (2013) 379–383.
[29] J.W. Phillips, S.A. Mumford, The dimorphism of certain aliphatic compounds. Part II, J. Chem. Soc. (1932) 898–906.
[30] J.W. Philips, S.A. Mumford, The dimorphism of certain aliphatic compounds. Part IV: the ethyl esters, Rec. Trav. Chim. Pays Bas 52 (1933) 181–194.
[31] M.G. Broadhurst, An analysis of the solid phase behavior of n-paraffins, J. Res. Natl. Bur. Stand. A. Phys. Chem. 66A (3) (1962) 241–249.
[32] E.B. Sirota, H.E. King Jr., D.M. Singer, H.H. Shao, Rotator phases of the normal alkanes: an X-Ray scattering study, J. Chem. Phys. 98 (1993) 5809–5824.
[33] J.C. Smith, Higher Aliphatic Compounds. Part II. The Systems Hexadecyl Iodide-octadecyl Iodide and Hexadecane-octadecane, The Dyson Perrins Laboratory, Oxford University, 1932, pp. 737–741.
[34] A. Genovese, G. Amarasinghe, M. Glewis, D. Mainwaring, R.A. Shanks, Crystallisation, melting, recrystallisation and polymorphism of n-eicosane for application as a phase change material, Thermochim. Acta 443 (2006) 235–244.
[35] P. Gill, T.T. Moghadam, B. Ranjbar, Differential scanning calorimetry techniques: applications in biology and nanoscience, J. Biomol. Tech. 21 (2010) 167–193.
[36] A.A. Kulkarni, B.Y. Zarah, K.D. Luks, J.P. Kohn, Phase-equilibria behavior of

system carbon dioxide + n-decane at low temperatures, J. Chem. Eng. Data 19 (1974) 92–94.

[37] S. Landa, J. Romovacek, H. Romovackova, Composition of low-temperature brown-coal I. Paraffins, Chem. Listy 49 (1955) 313.

[38] A. Müller, W. Borchard, Correlation between DSC curves and isobaric state diagrams. 3. Simulation of smeared DSC curves, J. Phys. Chem. B 101 (1997) 4307–4312.

[39] M. Hillert, Phase Equilibria, Phase Diagrams and Phase Transformations Their Thermodynamic Basis, second ed., Cambridge University Press, New York, 2008.

[40] N.D.D. Carareto, A.O. Santos, M.P. Rolemberg, L.P. Cardoso, M.C. Costa, A.J.A. Meirelles, On the solid–liquid phase diagrams of binary mixtures of even saturated fatty alcohols: Systems exhibiting peritectic, Thermochim. Acta 589 (2014) 137–147.

[41] M. Matsuoka, R. Ozawa, Determination of solid-liquid phase equilibria of binary organic systems by differential scanning calorimetry, J. Cryst. Growth 96 (1989) 596–604.

List of symbols

Latin letters

a: parameter in Eq. (2)
a_i^L: activity of compound *i* in liquid phase
a_i^S: activity in compound *i* in solid phase
b: parameter in Eq. (2) [K]
H: enthalpy [J mol^{-1}]
$\Delta_{fus}H_i$: enthalpy of fusion of compound *i* [J mol^{-1} or J g^{-1}]
K_{ij}: equilibrium constant of the peritectic reaction between compound i and j
R: gas constant [8.314 J mol^{-1} K^{-1}]
T: temperature [K]
T_f: fusion temperature [K]
T_e: eutectic temperature [K]
T_t: solid phase transition temperature [K]
v_i: molar volume of pure compound *i*
x_i: molar fraction of compound *i* in liquid phase

Greek letters

ϕ_i: volume fraction of compound *i*
χ_{ij}: Flory Huggins interaction parameter between compounds *i* and *j*